ELSEVIER

Surface Science 454–456 (2000) 968–973

surface science

www.elsevier.nl/locate/susc

Vibrational spectroscopy of CO adsorbed on supported ultra-small transition metal particles and single metal atoms

Martin Frank, Ralf Kühnemuth, Marcus Bäumer *, Hans-Joachim Freund

Fritz-Haber-Institut der Max-Planck-Gesellschaft, Faradayweg 4–6, D-14195 Berlin, Germany

Abstract

Ultra-small rhodium, palladium and iridium particles with minimum average sizes of five atoms have been grown on a thin, well-ordered alumina film at temperatures of 90 K and below. Scanning tunneling microscopy (STM) served to characterize the morphology of these deposits. In the infrared spectra of adsorbed carbon monoxide, characteristic features were observed by infrared reflection absorption spectroscopy (IRAS). These originate from CO adsorbed on single metal atoms and extremely small aggregates, most likely dimers or trimers. In this way, we have detected the atomic nuclei of heterogeneous rhodium nucleation at 90 K. Located at oxide point defects, these atoms form rhodium dicarbonyl species with a symmetric stretch frequency of 2117 cm^{-1}, while for iridium dicarbonyl species a frequency of 2107 cm^{-1} was found. At 60 K, rhodium aggregates also grow elsewhere on the oxide film. Comparing the nucleation behaviour at low temperatures, we find an increasing metal–oxide interaction strength in the order Pd < Rh < Ir.

Keywords: Adatoms; Aluminum oxide; Clusters; Iridium; Palladium; Rhodium; Surface defects; Vibrations of adsorbed molecules

1. Introduction

A considerable number of studies utilizing surface science techniques have dealt with metal particles on oxide single crystals or thin films, exploring their structural, electronic and chemisorption characteristics [1–6]. At extremely small sizes, their properties are expected to be strongly influenced by their interaction with the oxide substrate. Yet there is limited experimental information on subnanometre-sized particles or even single metal atoms on such supports.

In many cases, aggregates are prepared via growth from the gas phase at or above room temperature. Under these conditions, adatom diffusion lengths may be considerable for mid-to-late transition metals, resulting in relatively large aggregates. To access the subnanometre size regime, we have therefore utilized growth at and below liquid nitrogen temperatures as well as low metal exposures. As shown by scanning tunneling microscopy (STM), ultra-small rhodium, palladium and iridium particles with minimum sizes of five atoms have been prepared in this way. In this paper, we present infrared spectra of CO adsorbed on such deposits. These provide detailed information on the metal nucleation behaviour, which is related to the metal–oxide interaction strength.

2. Experimental

Experiments were performed in a multi-chamber ultrahigh vacuum (UHV) system with a base

* Corresponding author. Fax: +49-30-8413-4101.
E-mail address: baeumer@fhi-berlin.mpg.de (M. Bäumer)

0039-6028/00/$ - see front matter
PII: S0039-6028(00)00241-7

pressure below 2×10^{-10} mbar. The NiAl(110) crystal was mounted on a sample carrier which could be transferred between the various experimental stages. The crystal temperature was monitored by an NiCr/Ni thermocouple spot-welded to the sample.

STM images were taken with an Omicron variable-temperature scanning tunneling microscope, which was operated at room temperature in this study. Infrared spectra were acquired with a Bruker IFS 66v/S vacuum infrared spectrometer. A liquid-nitrogen-cooled MCT detector was used to detect the p-polarized light reflected from the sample surface at 84° grazing incidence. Typically, 1024 scans were accumulated. The spectral resolution after apodization was 3.3 cm^{-1}.

The alumina film was prepared via oxidation of the NiAl(110) single-crystal surface [7]; its quality was checked by STM as well as via its phonon bands in the infrared spectrum.

Metals (>99.9%) were evaporated from a rod via electron bombardment. During evaporation the sample was put on a retarding potential to avoid effects due to ions accelerated towards the sample. Flux calibration was performed with a quartz crystal microbalance as well as by two-dimensional submonolayer growth on NiAl(110) and subsequent STM measurements. Deposition rates varied between 0.11 and 0.25 monolayers (ML) per min (1 ML rhodium, palladium and iridium correspond to 1.60, 1.53 and 1.57×10^{15} atoms cm^{-2}, respectively). The samples were exposed to CO (AGA, >99.997%) and ^{13}CO (Cambridge Isotope Laboratories; >99% ^{13}C, >90% ^{16}O) utilizing a pin hole doser.

3. Results and discussion

Under control of the substrate temperature, metals were evaporated on to a thin, well-ordered alumina film grown on an NiAl(110) single-crystal surface [7]. At 300 K, rhodium [8,9] and palladium [6,9,10] decorate the network of rotational and antiphase domain boundaries separating long-range ordered domains of the oxide film [11]. At this temperature, iridium also nucleates within the domains [9]. This behaviour is found for all three metals at temperatures of 90 K and below [6,8–10].

The average number of atoms per particle was determined from the number of metal atoms deposited and the island density observed by STM. These tunneling measurements were performed after CO adsorption and heating to temperatures between 300 and 670 K. Below room temperature, diffusion of the smallest aggregates and single atoms cannot be ruled out. Therefore, the data given below constitute upper bounds for the particle sizes right after preparation. Further annealing to the maximum temperatures employed, however, did not lead to significant changes in the observed island number densities [6].

3.1. Rhodium deposits

The infrared spectrum taken from a rhodium deposit prepared and saturated with CO at 90 K (average particle size: nine atoms) is displayed in Fig. 1a (top). The most prominent feature in the stretching region of terminally bound CO molecules is a sharp, intense band at 2117 cm^{-1}. This signal has previously been shown to arise from isolated rhodium atoms bound to oxide defects [12]. Both the number of adsorbed CO molecules and the nature of the defect site remained unclear. Features at lower frequencies are assigned to molecules on rhodium aggregates.

In order to gain insight into the stoichiometry of the rhodium carbonyl species giving rise to the band at 2117 cm^{-1}, isotopic mixture experiments have been performed. If such a signal was due to RhCO, an equimolar mixture of ^{12}CO and ^{13}CO should result in the appearance of a second infrared band of equal intensity about 47 cm^{-1} lower. In the case of $Rh(CO)_2$, three species of different isotopic composition would be formed with relative abundancies of 1:2:1, giving rise to three infrared bands with intensities reflecting this ratio.

The latter observation is indeed made experimentally (Fig. 1a, bottom), thereby showing that $Rh(CO)_2$ is responsible for the infrared band under investigation. Such rhodium gem-dicarbonyl species, with an oxidation state of +1 assigned to the rhodium, result from the disruption of metal crystallites on technical Rh/Al_2O_3 catalysts (symmetric stretch: ~2100 cm^{-1}, asymmetric stretch: ~2035 cm^{-1}) [13–15]. They have also been

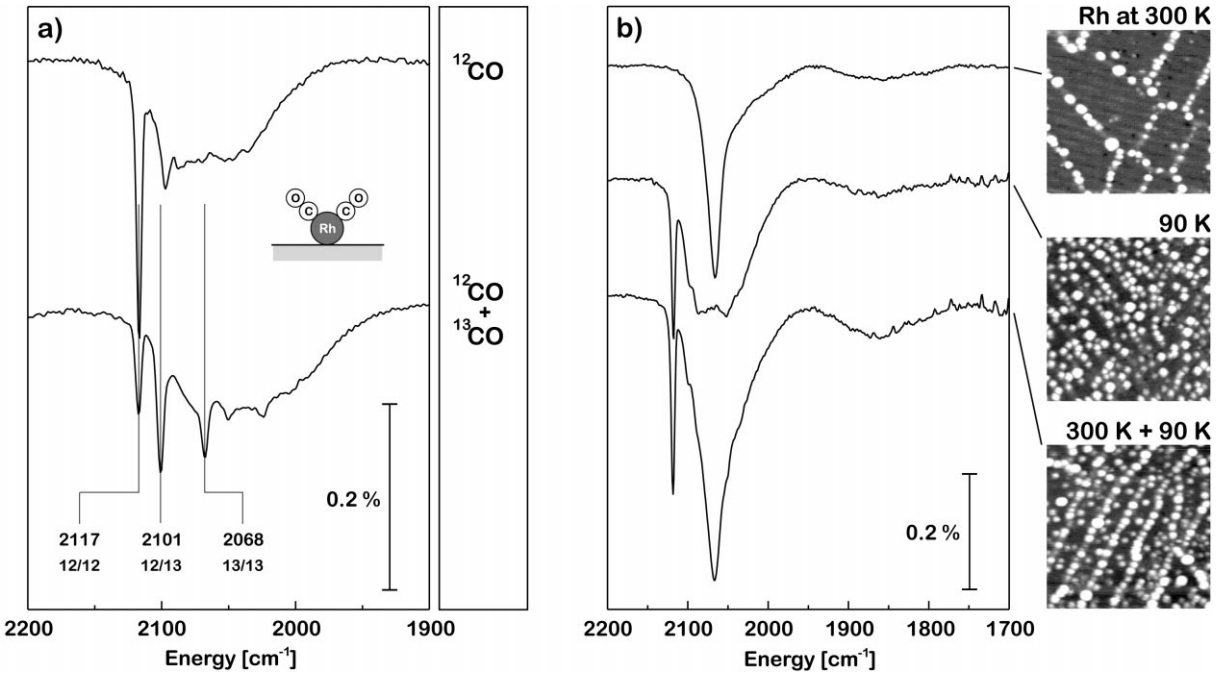

Fig. 1. (a) Infrared spectra taken after deposition of 0.028 ML of rhodium and subsequent saturation with ^{12}CO (top) and an approximately equimolar mixture of ^{12}CO and ^{13}CO (bottom) at 90 K. The isotopic compositions giving rise to the three dicarbonyl bands are indicated below the corresponding wavenumbers. Average particle size: nine atoms. (b) Infrared spectra recorded after CO saturation of rhodium deposits at 90 K, along with corresponding room-temperature STM images (500 Å × 500 Å). Top: 0.057 ML of rhodium deposited at 300 K. Middle: 0.057 ML of rhodium deposited at 90 K. Bottom: 0.057 ML of rhodium deposited at 300 K, followed by the same exposure at 90 K.

observed on $TiO_2(110)$ single crystals ($\sim$2110 cm^{-1}/$\sim$2030 cm^{-1}) [16,17], where a similar disruption process has been followed by STM [18].

From our data, no signal due to the antisymmetric stretch is discerned (Fig. 1a). Since for thin oxide films on metal substrates the surface selection rule applies, its dynamic dipole moment must be oriented parallel to the oxide surface.

We now turn to the type of rhodium nucleation site responsible for the infrared band at 2117 cm^{-1}. We first note that rhodium deposition at room temperature results in the formation of metal aggregates located at oxide domain boundaries. Upon CO saturation at 90 K, no $Rh(CO)_2$ is formed (Fig. 1b, top). As discussed above, this is in clear contrast to a low-temperature deposit. Nucleating inside the domains, it gives rise to the dicarbonyl band (Fig. 1b, middle). In fact, STM measurements revealed that point defects are the primary nucleation sites under these conditions [9]. Rhodium decoration of the line defects at room temperature *preceding* deposition at 90 K does *not* suppress rhodium dicarbonyl formation (Fig. 1b, bottom). Consequently, we may conclude that the $Rh(CO)_2$ species are not associated with the domain boundaries but with *oxide point defects*, which are the dominant rhodium nucleation sites at 90 K.

In order to reduce the particle sizes further, growth and adsorption studies were performed at 60 K. In the infrared spectrum of ^{12}CO adsorbed on such a rhodium deposit (average particle size at 300 K: five atoms) a number of distinct signals are observed at frequencies between 2172 and 1961 cm^{-1}, along with a broad absorption band in the range of 2120 to 1950 cm^{-1} (Fig. 2, bottom) and a very weak feature due to multiply coordinated CO at 1856 cm^{-1}.

As in the case of the 90 K deposits, the broad

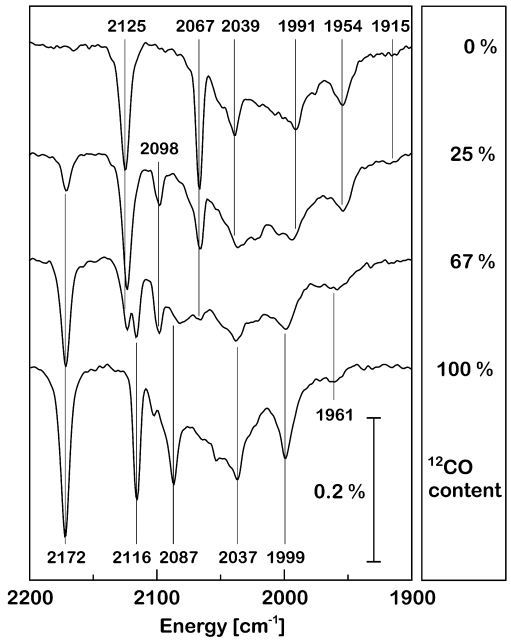

Fig. 2. Series of infrared spectra acquired at 60 K after deposition of 0.020 ML of rhodium at 60 K and subsequent saturation with isotopic mixtures of ^{12}CO and ^{13}CO at the same temperature. The percentage of ^{12}CO is given next to the spectra. Average particle size: five atoms.

band and the sharp feature at 2116 cm^{-1} are attributed to terminally bound CO on rhodium aggregates of various sizes and to $Rh(CO)_2$ species at oxide point defects, respectively. Physisorption on the Al_2O_3 itself [19] is reflected by the band at 2172 cm^{-1}, which is also observed upon CO exposure of the pristine oxide film.

One or more new types of rhodium nucleation site clearly come into play at 60 K compared with the 90 K situation. This is indicated by the observation of a smaller mean particle size, by the lower intensity of the infrared band due to rhodium nucleated at the point defects, and finally by the appearance of new signals at 2087, 2037, 1999 and 1961 cm^{-1}. Their small half-width points to the presence of uniform, isolated $Rh_n(CO)_m$ species. Similar features are obtained for deposits with even lower mean particle sizes. Therefore they most likely originate from atomic, dimeric or possibly trimeric rhodium.

Again, the use of isotopic mixtures provides additional information on the identity of the surface species. As expected, saturation with ^{13}CO results in a downward shift of the entire spectrum by 42 to 49 cm^{-1} (Fig. 2, top). Slight changes in relative band intensities are due to small variations in sample temperature. Following the spectral evolution with isotopic composition, differences in behaviour of the individual bands are observed (Fig. 2):

- as expected for single, isolated CO molecules, the intensities of the bands at 2172 and 2125 cm^{-1} vary linearly with the concentration of the corresponding isotopes;
- in line with the statistics of mixture, the rhodium dicarbonyl bands at 2116 and 2067 cm^{-1} are more strongly attenuated upon addition of the other isotope, and a band due to the mixed dicarbonyl is observed at 2098 cm^{-1};
- between the bands at 1999 and 1954 cm^{-1}, no such signal at an intermediate frequency is found, implying that they do not originate from rhodium dicarbonyl species at a different surface site. Their slow intensity variation may indicate RhCO; and
- in clear contrast to this, the 2087 cm^{-1} band vanishes completely upon admixture of 33% ^{13}CO. This is conceivable only if the surface complex contains three or more CO molecules.

The information gained from the other signals is less specific. In summary, however, we may conclude that several different types of rhodium particles are responsible for the infrared features observed. Presently, density-functional calculations on small rhodium carbonyls are in progress [20]. Calculated vibrational frequencies of such systems may help to identify the species present on the alumina film.

3.2. Iridium and palladium deposits

These studies on small rhodium particles have been extended to include neighbouring elements in the Periodic Table. Infrared spectra recorded after deposition of comparable amounts of palladium, rhodium and iridium, and subsequent CO saturation at 90 K, are displayed in Fig. 3. We note differences in the low-wavenumber region, where vibrational frequencies of molecules in multiply coordinated sites are located. As on single crystals,

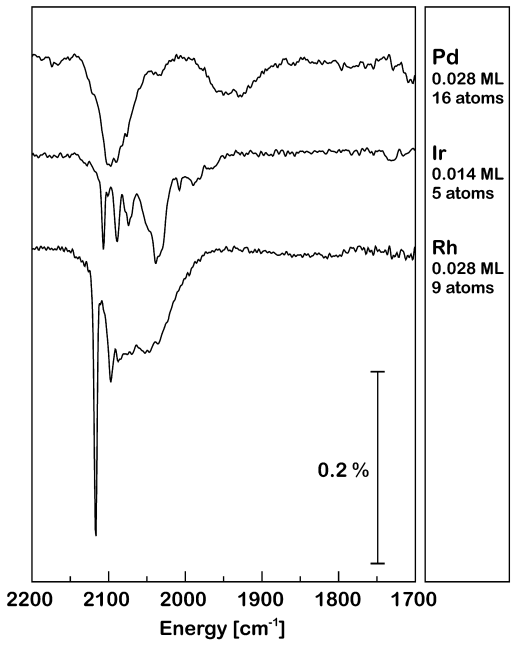

Fig. 3. Infrared spectra of palladium, iridium and rhodium deposited at 90 K and saturated with CO at the same temperature.

the population of such sites is highest on palladium [21,22], while no such CO is observed on iridium [23,24].

The differences in the region of terminally bound CO, however, are much more pronounced. In the case of iridium, several distinct features are observed. In analogy to the $Rh(CO)_2$ band at 2117 cm^{-1}, the sharp signal at 2107 cm^{-1} may be attributed to $Ir(CO)_2$ species via isotopic mixture experiments (not shown). Bands with similar frequencies have been assigned to the symmetric stretch of $Ir^+(CO)_2$ on technical Ir/Al_2O_3 catalysts (2107–2090 cm^{-1}) [25] and on the iridium-loaded zeolite H-ZSM-5 (2104 cm^{-1}) [26]. The appearance of a number of bands at lower wavenumber is reminiscent of the 60 K rhodium deposits (Fig. 2), pointing to a comparable nucleation behaviour.

By contrast, no signs of atomically disperse palladium or of structurally well-defined aggregates are observed. Indeed, the infrared spectrum is rather similar to that observed on much larger, disordered palladium aggregates [27]. At the same metal exposure, the palladium particles are found to be larger than the rhodium aggregates by room-temperature STM (Fig. 3).

Our observations show that the infrared spectra of adsorbed CO provide valuable information on the size of metal nanoparticles. In the nucleation regime the metal particle size increases from iridium across rhodium to palladium, implying the opposite trend in metal–oxide interaction strength.

4. Summary and conclusion

We have shown that subnanometre-sized transition metal particles may be prepared on a thin alumina film via growth at temperatures of 90 K and below. Upon saturation with CO, extremely small aggregates give rise to characteristic signatures in the stretching region of the infrared spectrum. Utilizing isotopically labelled CO, information on the composition of the resulting carbonyl species may be extracted. Consequently, infrared spectroscopy constitutes a tool to study the nucleation behaviour of metals on oxide substrates.

We have identified $Rh(CO)_2$, originating from the atomic rhodium nuclei at oxide point defects at 90 K, with a symmetric stretch frequency of 2117 cm^{-1}, while for $Ir(CO)_2$ a frequency of 2107 cm^{-1} was found. These values resemble those observed for metal dicarbonyl species on technical catalysts and oxide single crystals.

At 60 K, additional types of rhodium nucleation site result in a further reduction of particle size and in a correspondingly complex infrared spectrum. Judging from their nucleation behaviour at 90 K, the interaction between the admetals and the alumina substrate increases in the order palladium < rhodium < iridium, in line with the heats of formation of the corresponding metal oxides.

Acknowledgements

For financial support of our work, we are grateful to a number of agencies: Deutsche Forschungsgemeinschaft (DFG), Bundesminis-

terium für Bildung und Forschung (BMBF), Fonds der Chemischen Industrie and NEDO International Joint Research Grant on Photon and Electron Controlled Surface Processes. This work was also supported in part by Synetix, a member of the ICI group, through their Strategic Research Fund. M.F. thanks the Studienstiftung des deutschen Volkes for a fellowship. Finally, we would like to thank Professor N. Russo and Dr T. Mineva for valuable discussions.

References

[1] D.W. Goodman, Chem. Rev. 95 (1995) 523.
[2] H.-J. Freund, Angew. Chem. Int. Ed. Engl. 36 (1997) 452.
[3] C.T. Campbell, Surf. Sci. Rep. 27 (1997) 1.
[4] R.M. Lambert, G. Pacchioni (Eds.), Chemisorption and Reactivity on Supported Clusters and Thin Films, NATO ASI Series, Series E, vol. 331, Kluwer Academic Publishers, Dordrecht, 1997.
[5] C.R. Henry, Surf. Sci. Rep. 31 (1998) 231.
[6] M. Bäumer, H.-J. Freund, Prog. Surf. Sci. 61 (1999) 127.
[7] R.M. Jaeger, H. Kuhlenbeck, H.-J. Freund, M. Wuttig, W. Hoffmann, R. Franchy, H. Ibach, Surf. Sci. 259 (1991) 235.
[8] M. Bäumer, M. Frank, J. Libuda, S. Stempel, H.-J. Freund, Surf. Sci. 391 (1997) 204.
[9] M. Bäumer, M. Frank, M. Heemeier, R. Kühnemuth, S. Stempel, H.-J. Freund, Surf. Sci 454–456 (2000) 957, these proceedings.
[10] M. Bäumer, J. Libuda, A. Sandell, H.-J. Freund, G. Graw, Th. Bertrams, H. Neddermeyer, Ber. Bunsenges. Phys. Chem. 99 (1995) 1381.
[11] J. Libuda, F. Winkelmann, M. Bäumer, H.-J. Freund, Th. Bertrams, H. Neddermeyer, K. Müller, Surf. Sci. 318 (1994) 61.
[12] M. Frank, R. Kühnemuth, M. Bäumer, H.-J. Freund, Surf. Sci. 427–428 (1999) 288.
[13] J.T. Yates Jr., T.M. Duncan, S.D. Worley, R.W. Vaughan, J. Chem. Phys. 70 (1979) 1219.
[14] P. Basu, D. Panayotov, J.T. Yates Jr., J. Am. Chem. Soc. 110 (1988) 2074.
[15] F. Solymosi, H. Knözinger, J. Chem. Soc. Faraday Trans. 86 (1990) 389.
[16] J. Evans, B. Hayden, F. Mosselmans, A. Murray, Surf. Sci. 279 (1992) L159.
[17] J. Evans, B. Hayden, F. Mosselmans, A. Murray, Surf. Sci. 301 (1994) 61.
[18] A. Berkó, F. Solymosi, J. Catal. 183 (1999) 91.
[19] R.M. Jaeger, J. Libuda, M. Bäumer, K. Homann, H. Kuhlenbeck, H.-J. Freund, J. Electron Spectrosc. Relat. Phenom. 64/65 (1993) 217.
[20] T. Mineva, N. Russo, private communication.
[21] P. Uvdal, P.-A. Karlsson, C. Nyberg, S. Andersson, N.V. Richardson, Surf. Sci. 202 (1988) 167.
[22] T. Gießel et al., Surf. Sci. 406 (1998) 90.
[23] G. Kisters, J.G. Chen, S. Lehwald, H. Ibach, Surf. Sci. 245 (1991) 65.
[24] J. Lauterbach, R.W. Boyle, M. Schick, W.J. Mitchell, B. Meng, W.H. Weinberg, Surf. Sci. 350 (1996) 32.
[25] F. Solymosi, É. Novák, A. Molnár, J. Phys. Chem. 94 (1990) 7250.
[26] T.V. Voskobojnikov, E.S. Shpiro, H. Landmesser, N.I. Jaeger, G. Schulz-Ekloff, J. Mol. Catal. A - Chem. 104 (1996) 299.
[27] K. Wolter, O. Seiferth, H. Kuhlenbeck, M. Bäumer, H.-J. Freund, Surf. Sci. 399 (1998) 190.